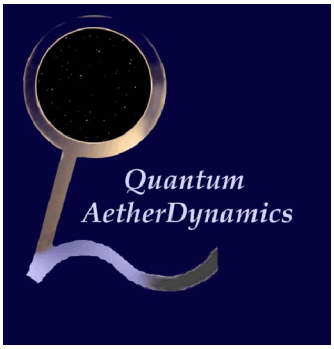

Quantum AetherDynamics Institute (QADI)

Ledger-One Longitudinal Closure from SiC Raman LOPC: DSF+MCR Resolving-Power Protocol and Literature Reanalysis

David W. Thomson III
Quantum AetherDynamics Institute (QADI), Alma, Illinois, USA
ORCID: 0000-0002-5830-5427

Version 1.0 – January 27, 2026

This article is published by the Quantum AetherDynamics Institute (QADI).

It develops the Aether Physics Model (APM)

Abstract

Raman longitudinal optical phonon–plasmon coupled (LOPC) features in SiC are widely used as empirical carrier-density and resistivity proxies, but multilayer wafers and finite depth of field convolute spectral responses and reduce such workflows to regression without falsifiable invariants. This paper upgrades SiC LOPC metrology to a ledger-first closure test in Quantum Measurement Units (QMU) by normalizing Raman observables into dimensionless QMU form and enforcing the Aether Rotational Self-Identity (Ledger One) as the propagation anchor. Two closure targets are defined: (i) a spectrum-only invariant based on a QMU-normalized LOPC inversion combined with a linewidth-normalized quotient, and (ii) a transport-coupled invariant that incorporates a unitless resistivity proxy. A decisive resolving-power experiment is then specified: mixed bulk depth spectra should fail closure as depth varies, while multivariate curve resolution (MCR) component spectra extracted from Dual Spatial Filtration (DSF) depth stacks should satisfy closure within uncertainty when they correspond to physical layers. Where raw spectral matrices are unavailable, a published feature-space proxy closure coordinate is constructed from reported intensity ratios and linewidths, enabling the same bulk-versus-component falsification on industrial datasets. A depth-axis modulation bound is extracted (in SI-free, unitless form) from open supplementary depth-of-analysis tables in a quantified Raman–eddy-current resistivity mapping study of 4H–SiC.

Keywords: QMU; APM; Ledger One; SiC; Raman spectroscopy; LOPC; DSF; MCR; closure invariants; resistivity mapping; depth profiling

1 Introduction

The Raman applications eBook documents that SiC polymorphs, carrier density, and multilayer depth structure can be evaluated by Raman spectroscopy; critically, it also states that Dual Spatial Filtration (DSF) improves depth resolution and that multivariate curve resolution (MCR) can deconvolve mixed spectra so that component (layer) carrier densities can be evaluated [JASCO, 2022]. The physics opportunity is to elevate such workflows from empirical calibration to a falsifiable closure test: do longitudinal Raman observables (LOPC center shift and damping) obey a dimensionless invariant when expressed in QMU and anchored to Ledger One?

Industrial and metrology datasets frequently publish feature tables and regression coefficients but withhold raw spectra. Calà *et al.* provide a high-value example in 4H–SiC: quantified Raman features of the LOPC region are used to predict eddy-current resistivity maps, and supplementary materials include a depth-of-analysis table plus explicit feature definitions and regression coefficients [Calà et al., 2025a,b,c]. These materials are sufficient to (i) state a decisive DSF+MCR closure experiment and (ii) build unitless, QMU-normalized closure coordinates that a data-holder can compute on either bulk spectra or MCR components.

To keep the main text ledger-clean, all reporting is in QMU-normalized and dimensionless form. Numerical values inherited from the literature are reduced to unitless ratios rather than reproduced in SI.

2 Ledger Closure Check

Ledger One (Aether Rotational Self-Identity). Define Ledger One as the fundamental QMU dimensional identity for Aether rotation:

$$A_u\,\mathrm{curl} = {F_q}^2\,{\lambda_C}^2.$$

This identity represents the Aether Rotational Self-Identity. Explicitly, it corresponds to the equation

$$A_u \cdot \mathrm{curl} = {F_q}^2 {\lambda_C}^2.$$

Using the mainstream anchor $F_q\,\lambda_C = c$, Ledger One may be recognized as

$$A_u \cdot \mathrm{curl} = c^2.$$

With Maxwell correspondence $c^2 = 1/(\mu_0\varepsilon_0)$, Ledger One is read as the QMU decomposition of the electromagnetic propagation constant into rotational (Aether unit A_u) and torsional (curl) geometries.

Ledger One is the only external anchor used here: once Raman observables are mapped into QMU, all closure statements are expressed as dimensionless invariants.

3 QMU normalization of Raman observables

Raman spectra are reported on a spatial-frequency axis (wavenumber shift). Let κ denote the Raman spatial frequency (dimension 1/length). QMU normalization is immediate:

$$\Omega := \frac{\omega}{F_q} = \lambda_C\,\kappa,$$

because $\omega = c\,\kappa$ and $c = F_q\lambda_C$. Thus every Raman peak position maps to a dimensionless QMU coordinate Ω by multiplication with λ_C.

Likewise, a linewidth (FWHM) $\Delta\kappa$ maps to a dimensionless damping proxy

$$\gamma := \lambda_C\,\Delta\kappa.$$

When only plotted linewidths are available, γ may be taken as a ratio to a within-study reference linewidth; the resulting γ remains unitless and preserves the closure logic.

Carrier density is naturally "per volume." With $\mathrm{volm} = {\lambda_C}^3$, define the dimensionless occupancy

$$n^* := n\,\mathrm{volm},$$

the carrier count per quantum volume.

4 LOPC longitudinal channel as a closure probe

In a polar semiconductor, free-carrier collective motion (plasmon) couples to the LO phonon through the longitudinal electric field, producing a Raman-active LOPC response. The eBook summarizes the key empirical monotonicity used in practice for SiC: only the L^+ branch is typically observed, it shifts to higher wavenumber with increasing carrier density, and its spectral shape broadens [JASCO, 2022]. Here, those same observables are treated as a longitudinal channel suitable for closure testing.

4.1 QMU LOPC inversion

In a minimal undamped polar-semiconductor model, longitudinal modes satisfy $\varepsilon(\omega) = 0$ with

$$\varepsilon(\omega) = \varepsilon_\infty \left(1 + \frac{\omega_{LO}^2 - \omega_{TO}^2}{\omega_{TO}^2 - \omega^2} - \frac{\omega_p^2}{\omega^2}\right),$$

where ω_p is the plasmon scale. Expressing all frequencies in QMU form ($\Omega = \omega/F_q$) yields an algebraic inversion for a dimensionless plasmon proxy in terms of measured peak centers:

$$\Omega_p^2 = \frac{\Omega_{L+}^2 \left(\Omega_{L+}^2 - \Omega_{LO}^2\right)}{\Omega_{L+}^2 - \Omega_{TO}^2}. \tag{1}$$

This conversion is ledger-first: it introduces no $\hbar$ and depends only on the propagation anchor $F_q\lambda_C$, already fixed by Ledger One.

4.2 Closure targets

Two closure targets are useful.

(i) Spectrum-only closure. Define the spectrum-only closure metric

$$\Xi \;:=\; \frac{\Omega_p^2}{\gamma}. \tag{2}$$

This requires only peak centers and linewidths and no external carrier density or resistivity.

(ii) Transport-coupled closure. When a transport proxy is available (eddy-current resistivity, four-point mapping, or a vendor map), define a unitless resistivity coordinate ρ^* by normalizing within the dataset (e.g., $\rho^* = \rho/\langle\rho\rangle$ for a fixed wafer point across a depth/NA sweep, or $\rho^* = \rho/\bar{\rho}$ across a lateral map at fixed objective). Then define

$$\Xi_\rho \;:=\; \rho^* \frac{\Omega_p^2}{\gamma}. \tag{3}$$

If Ξ_ρ collapses more tightly than ρ^* alone, the longitudinal spectral observables compress three-dimensional transport variability into a single closed longitudinal degree of freedom.

Ledger One enters here by forbidding spurious scale factors: the only allowed propagation product is $F_q\lambda_C$, and the only allowed geometric split of that propagation scale is $A_u$curl.

5 DSF+MCR as a resolving-power experiment

The eBook states directly that DSF offers significantly higher spatial resolution for depth profiling and that MCR can deconvolve mixed spectra so that each component spectrum (layer) can be evaluated [JASCO, 2022]. In the closure-test framing, DSF+MCR is not merely a data-cleaning step; it is a resolving-power experiment with a binary physics criterion.

Let $X(z,\Omega)$ be the measured DSF depth stack (bulk spectra at depth settings z). MCR-ALS seeks

$$X(z,\Omega) \;\approx\; \sum_{j=1}^{N_c} C_j(z)\, S_j(\Omega),$$

with $C_j(z) \geq 0$ and $S_j(\Omega) \geq 0$.

5.1 Definitive criterion (bulk fails, components pass)

A definitive resolving-power demonstration is the existence of a closure functional $\mathcal{K}[\cdot]$ such that:

> *Bulk closure failure:* $\mathcal{K}[X(z,\cdot)]$ varies significantly with z.
> *Component closure:* for each recovered component j, $\mathcal{K}[S_j]$ is component-constant (and stable under bootstrap/initialization variations) on the depth intervals where $C_j(z)$ dominates.

In this paper, $\mathcal{K}$ is instantiated by Ξ (preferred, because it is spectrum-only; Section 4.1) and by Ξ_ρ when a unitless transport proxy exists (Eq. (3)). Where full spectral matrices are withheld, $\mathcal{K}$ can be instantiated by a published feature-space proxy (next section).

Operationally, the pass/fail logic is statistical:

$$\mathrm{Var}\big(\Xi_{\mathrm{bulk}}(z)\big) \;\gg\; \mathrm{Var}\big(\Xi_j(z)\,|\,C_j(z) > \tau\big),$$

for a dominance threshold τ that excludes depths where the component contribution is negligible. The same form applies to Ξ_ρ and to any feature-space proxy closure coordinate.

6 Published depth-axis modulation bound in 4H–SiC

Calà *et al.* intercalibrate quantified Raman features against noncontact eddy-current resistivity measurements in 4H–SiC wafers and provide supplementary depth-of-analysis predictions for multiple microscope objectives at two wafer points [Calà et al., 2025a,b]. Their ESI Table 4 lists, for each objective, the numerical aperture (NA), an estimated depth of resolution d_f, and a model-predicted resistivity at two map points.

To keep the present paper SI-free, we normalize each quantity to form unitless vectors:

$$d_f^* := \frac{d_f}{\max(d_f)}, \qquad \rho^* := \frac{\rho}{\langle\rho\rangle_{\mathrm{depth}}},$$

where the averaging is performed separately for each wafer point across the objective list. Table 1 reports these unitless ratios computed from their supplementary table.

Two physics-relevant bounds follow immediately:

(i) The depth-axis resistivity modulation at fixed lateral position is modest but nonzero. The unitless span factors are

$$\max(\rho^*)/\min(\rho^*) \approx 1.053 \quad \text{(point 1–8)}, \qquad \max(\rho^*)/\min(\rho^*) \approx 1.062 \quad \text{(point 5–2)}.$$

Table 1: Unitless depth-axis modulation extracted from the supplementary depth-of-analysis table in Calà et al. [2025b]. Values are normalized within the table; no SI values are reproduced.

Objective	d_f^*	ρ^* (point 1–8)	ρ^* (point 5–2)
100×	0.0776	0.9968	0.9679
80×	0.1116	0.9924	0.9838
50×	0.2503	1.0211	0.9962
20×	0.3901	1.0200	1.0280
10×	1.0000	0.9698	1.0240

(ii) The modulation is nonprogressive in d_f^* contradicting the hypothesis of a simple surface-to-bulk gradient.

These bounds motivate the closure test: if ρ^* varies with the depth kernel, then the longitudinal spectral observables (Ω_p^2 and γ) must co-vary so that Ξ_ρ remains constant if the longitudinal channel is closed. Calà *et al.* explicitly use LOPC position/width and intensity ratios as predictors in their regression model [Calà et al., 2025a,b,c]; therefore, a data-holder can compute Ξ_ρ on the same objective/depth sweep once the corresponding LOPC parameters are tabulated or digitized.

7 Feature-space proxy closure from published deconvolution workflows

Industrial datasets often withhold raw spectra but publish deconvolved feature definitions and regression coefficients. Calà *et al.* provide such a set: the LOPC region is deconvolved into two bands at approximately 838 and 964 (their $p5$ axial and $p6$ planar modes), and the workflow uses relative band heights and FWHM values to predict resistivity [Calà et al., 2025a,b]. Two points are essential for a unit-free closure coordinate:

(i) intensities are not used absolutely; they are ratios to a strong reference band (their $p3$), hence pure numbers [Calà et al., 2025b]; (ii) predictors are autoscaled (mean-subtracted and divided by standard deviation) before regression [Calà et al., 2025c].

Define $H_5 := I_{p5}/I_{p3}$ and $H_6 := I_{p6}/I_{p3}$ (pure numbers) and let W_5, W_6 denote the corresponding linewidth features (used as unitless ratios or mapped into QMU by $W^* = \lambda_C\,\Delta\kappa$ when available). Let $\widehat{H}_5, \widehat{H}_6, \widehat{W}_5, \widehat{W}_6$ denote autoscaled predictors on any dataset to be analyzed.

Calà *et al.* publish regression coefficients for these four predictors [Calà et al., 2025c]. A unit-free *transport coordinate* can be formed by normalizing all weights to the magnitude of the $\widehat{W}_6$ coefficient:

$$\Psi \;:=\; 0.718\,\widehat{H}_5 \;+\; 0.424\,\widehat{H}_6 \;+\; 0.721\,\widehat{W}_5 \;-\; 1.000\,\widehat{W}_6. \tag{4}$$

The numerical factors are coefficient ratios and therefore pure numbers derived from the published model summary.

7.1 Using Ψ for the definitive DSF+MCR proof

Even when raw spectra are withheld, a lab holding DSF depth stacks can compute H_5, H_6, W_5, W_6 at each depth, run MCR on the depth stack, and evaluate (4) on both:

$$\Psi_{\text{bulk}}(z) \text{ from bulk fits of } X(z,\cdot), \qquad \Psi_j(z) \text{ from fits of reconstructed } C_j(z)S_j(\cdot).$$

The definitive resolving-power claim becomes:

$$\text{Var}(\Psi_{\text{bulk}}(z)) \;\gg\; \text{Var}(\Psi_j(z)\,|\,C_j(z) > \tau),$$

for each component j and a sensible dominance threshold τ. If the inequality holds, DSF+MCR is demonstrated to convert mixed spectra into layer-resolved components with closed transport coordinates. If it fails, the failure localizes additional physics (polytype mixing, compensation gradients, defect populations, or photo-generated carriers).

8 4H/6H polytype indexing and MCR separation

Calà *et al.* restricted their regression model to 4H–SiC because additional polytype bands disrupt a fixed-window model [Calà et al., 2025a]. The closure formulation here is stronger: *each polytype defines its own longitudinal closure constant set.* Operationally, the correct extension to 6H–SiC is not to force a 4H window onto 6H spectra, but to (i) use polymorph discrimination to tag polytype, then (ii) fit an appropriate LOPC basis within each tag and compute Ξ, Ξ_ρ, and/or Ψ within that tagged basis. The resulting test is crisp: closure should hold within a polytype and exhibit discrete shifts (not continuous drift) when the polytype tag changes. In mixed-polytype wafers, MCR is expected to separate polytype-specific spectra into distinct components, enabling per-component closure rather than bulk regression failure.

9 Minimum dataset needed from data holders

To execute the definitive proof (bulk fails, components pass), a data holder need only provide (or privately share) a minimal matrix:

- a DSF depth stack of Raman spectra in the LOPC window (e.g. ~ 750 to ~ 1050 on the wavenumber axis), at $N_z \gtrsim 20$ depth settings;
- the fitting convention for extracting L^+ center and linewidth (and LO/TO references), or equivalently the deconvolution feature definitions H_5, H_6, W_5, W_6;
- optional: any independent layer annotation (expected epi/substrate boundaries) for interpretability only.

No SI reporting is required for the closure plots: the entire analysis can be conducted in QMU dimensionless variables (Ω, γ) and pure intensity ratios (H_5, H_6).

10 Discussion and predictions

The scientific value added to the eBook is a falsifiable closure target. Instead of using LOPC observables only as regressors for carrier density or resistivity, we treat them as a longitudinal channel that must satisfy ledger-compatible invariants when written in QMU and anchored to Ledger One.

Three outcomes are possible, and each is scientifically informative:

1. **Closure succeeds on MCR components.** Bulk spectra show depth-dependent drift in Ξ (and Ψ), but each component collapses to a tight cluster on its dominance interval. This is the definitive proof of DSF+MCR resolving power in ledger space.
2. **Closure fails even on components.** The layer itself is not a single transport state (compensation gradients, defect populations, photo-generated carriers). The failure is new diagnostic physics, not a mere replot.
3. **Polytype-indexed closure.** Within each polytype tag closure holds, but mixtures fail. This converts polytype discrimination from "classification" into a quantitative closure constraint.

The published supplementary depth-of-analysis table already supplies a unitless modulation bound on transport variability at fixed lateral points. The next literature-only step is to extract (digitize or tabulate) the corresponding LOPC position and linewidth parameters at the same objective settings and evaluate whether Ξ_ρ is more invariant than ρ^* alone. The next experimental step is for data holders to run the DSF+MCR closure proof on a small depth stack (dozens of spectra), reporting only QMU-normalized and dimensionless results.

Acknowledgments

The Quantum AetherDynamics Institute (QADI) is a private 501(c)(3) research institute developing the Aether Physics Model (APM) and Quantum Measurement Units (QMU) Thomson III [2025]. Publications and data are archived with DOIs in the AetherPhysics Zenodo community: zenodo.org/communities/aetherphysics.

References

Elisa Calà, Simone Cerruti, Cristina Sanna, Marco Maffè, Wen Chin Hsu, Man Hsuan Lin, Luciano Ramello, and Giorgio Gatti. Resistivity mapping of SiC wafers by quantified Raman spectroscopy. *Physical Chemistry Chemical Physics*, 27:13884–13892, 2025a. doi: 10.1039/D4CP04545A. URL https://doi.org/10.1039/D4CP04545A.

Elisa Calà, Simone Cerruti, Cristina Sanna, Marco Maffè, Wen Chin Hsu, Man Hsuan Lin, Luciano Ramello, and Giorgio Gatti. Electronic supplementary information (1): depth-of-analysis table, peak definitions, and feature statistics for "Resistivity mapping of SiC wafers by quantified Raman spectroscopy". Supplementary information PDF, 2025b. URL https://www.rsc.org/suppdata/d4/cp/d4cp04545a/d4cp04545a1.pdf. Supplementary information associated with the main article DOI: 10.1039/D4CP04545A.

Elisa Calà, Simone Cerruti, Cristina Sanna, Marco Maffè, Wen Chin Hsu, Man Hsuan Lin, Luciano Ramello, and Giorgio Gatti. Electronic supplementary information (2): regression model coefficients for "Resistivity mapping of SiC wafers by quantified Raman spectroscopy". Supplementary information PDF, 2025c. URL https://www.rsc.org/suppdata/d4/cp/d4cp04545a/d4cp04545a2.pdf. Supplementary information associated with the main article DOI: 10.1039/D4CP04545A.

JASCO. Raman spectroscopy: Application ebook. Corporate application eBook (PDF), October 2022. URL https://jascoinc.com/wp-content/uploads/2022/11/RamanApplicationEBook_US-sm.pdf. Landing page: https://www.jasco-global.com/application-ebook-raman-spectroscopy/.

David W. Thomson III. Quantum aetherdynamics institute (qadi): Community doi overview and citation guide. Zenodo, 2025. URL https://doi.org/10.5281/zenodo.17479314.